NASA TECHNICAL MEMORANDUM

NASA TM X-2999

NASA TM X-2999



# PERFORMANCE OF GAS-LUBRICATED CRUCIFORM-MOUNTED TILTING-PAD JOURNAL BEARINGS AND A DAMPED FLEXIBLY MOUNTED SPIRAL-GROOVE THRUST BEARING

*by Lloyd W. Ream*

*Lewis Research Center*
*Cleveland, Ohio 44135*

NATIONAL AERONAUTICS AND SPACE ADMINISTRATION • WASHINGTON, D. C. • MARCH 1974

| 1. Report No. | 2. Government Accession No. | 3. Recipient's Catalog No. |
|---|---|---|
| NASA TM X-2999 | | |

| 4. Title and Subtitle | 5. Report Date |
|---|---|
| PERFORMANCE OF GAS-LUBRICATED CRUCIFORM-MOUNTED TILTING-PAD JOURNAL BEARINGS AND A DAMPED FLEXIBLY MOUNTED SPIRAL-GROOVE THRUST BEARING | MARCH - 1974 |
| | 6. Performing Organization Code |

| 7. Author(s) | 8. Performing Organization Report No. |
|---|---|
| Lloyd W. Ream | E-7675 |
| | 10. Work Unit No. 502-25 |

| 9. Performing Organization Name and Address | 11. Contract or Grant No. |
|---|---|
| Lewis Research Center<br>National Aeronautics and Space Administration<br>Cleveland, Ohio 44135 | |
| | 13. Type of Report and Period Covered |
| 12. Sponsoring Agency Name and Address | Technical Memorandum |
| *National Aeronautics and Space Administration*<br>Washington, D.C. 20546 | 14. Sponsoring Agency Code |

15. Supplementary Notes

16. Abstract

A test program was conducted to determine the performance characteristics of gas-lubricated cruciform-mounted tilting-pad journal bearings and a damped spiral-groove thrust bearing designed for the Brayton cycle rotating unit (BRU). Hydrostatic, hybrid (simultaneously hydrostatic and hydrodynamic), and hydrodynamic tests were conducted in argon gas at ambient pressure and temperature ranges representative of operation to the 10.5 $kW_e$ BRU power-generating level. Performance of the gas lubricated bearings is presented including hydrostatic gas flow rates, bearing clearances, bearing temperatures, and transient performance.

17. Key Words (Suggested by Author(s))

Brayton rotating unit; Cruciform tilling pad gas bearings; Damped spiral groove thrust bearing.

18. Distribution Statement

Unclassified - unlimited

Cat. 15

| 19. Security Classif. (of this report) | 20. Security Classif. (of this page) | 21. No. of Pages | 22. Price* |
|---|---|---|---|
| Unclassified | Unclassified | 23 | $2.75 |

* For sale by the National Technical Information Service, Springfield, Virginia 22151

# PERFORMANCE OF GAS-LUBRICATED CRUCIFORM-MOUNTED TILTING-PAD JOURNAL BEARINGS AND A DAMPED FLEXIBLY MOUNTED SPIRAL-GROOVE THRUST BEARING

by Lloyd W. Ream

Lewis Research Center

## SUMMARY

A test program was conducted to determine the performance characteristics of gas-lubricated, cruciform-mounted, tilting-pad journal bearings and a damped spiral-groove thrust bearing designed for the Brayton cycle rotating unit (BRU). Hydrostatic, hybrid (simultaneously hyrostatic and hydrodynamic), and hydrodynamic tests were conducted in argon gas at ambient pressure and temperature ranges representative of operation to the 10.5-electrical-kilowatt BRU power-generating level. The first phase of testing of these gas bearings was to determine the hydrostatic performance, that is, the jacking gas flow and the lift capability. The required total flow to the bearings was $8.4\times10^{-3}$ kilogram per second ($1.85\times10^{-2}$ lb/sec) at 6-electrical-kilowatt ambient conditions. During hydrostatic operations, lifting of the shaft away from the bearings occurred when the ratio between supply pressure and ambient pressure exceeded values of 6.6 and 7 for ambient conditions of 10.2 and 13.6 newtons per square centimeter absolute (15 and 20 psia), respectively. The second phase of testing was to operate the bearings in a hybrid mode to locate the critical speeds and instabilities. The largest shaft orbit diameter obtained was 30 micrometers (1.2 mils) at 4770 rpm. The cruciform-mounted journal bearing and the friction-damped thrust bearing did not exhibit any instability during the transition from zero to rated speed. The third phase of the testing was to operate the bearings at the 6-electrical-kilowatt power level to measure their self-acting behavior at rated speed. The gas film of the journal bearings was 13 micrometers (0.5 mil). The maximum circular orbit of the shaft was 5 micrometers (0.2 mil) in diameter measured at the compressor-bearing end of the shaft. In the hydrodynamic mode the steady-state temperature reached by the bearings is comparable with the temperature reached in a hot BRU, except for the loaded side of the thrust bearing. The temperature measured on the loaded side of the thrust bearing was about 15 percent higher than the temperature measured on the prototype Rayleigh step thrust bearing.

## INTRODUCTION

The NASA Lewis Research Center is investigating the technology required for a Brayton cycle system for electrical power generation. As part of the supporting bearing program, alternate Brayton rotating unit (BRU) gas bearings were designed and fabricated by Mechanical Technology Incorporated of Latham, New York; they are fully described in reference 1. One set of these bearings, consisting of nonconforming pivoted-pad journal bearings and an undamped spiral-groove thrust bearing, was installed at Lewis in a BRU dynamic simulator. The experimental evaluation is reported in reference 2. The second unit, consisting of cruciform tilting-pad journal bearings and a damped flexibly mounted spiral-groove thrust bearing, was also installed in the same dynamic simulator and experimentally evaluated. The results of this test are presented in this report.

Reference 3 describes the BRU power system for which the bearings are designed. Reference 4 describes the BRU dynamic simulator in which the bearings were installed and tested. Basically, the tests were made to determine the bearing load capacity characteristics. Argon was used as the bearing lubricant, and air was used to drive the turbine.

Three modes of testing were used for this bearing evaluation. The first mode (hydrostatic) applies jacking gas to the bearings, controls the housing pressure, and allows zero rotation of the shaft. The second mode (hybrid) adds shaft rotation to the hydrostatic mode. This is achieved by spinning up the shaft to rated speed with the air-driven turbine. The third mode (hydrodynamic) is a self-acting operation. This mode of operation of the bearings was accomplished by slowly removing the jacking gas supply from the bearings until they operated on the gas film that they themselves generated.

Although the primary units are in the SI system, the work was performed in the U.S. customary system of units.

## BEARING DESIGN

The condition under which the gas bearings were designed to operate are as follows:

| | |
|---|---|
| Rotor speed, rpm | 36 000 |
| Rotor weight, kg (lb) | 99.9 (21.8) |
| Lubricant | Helium-xenon (molecular weight, 83.8) |
| Viscosity, N sec/$m^2$ (poise) | $3.52\times10^{-5}$ at 172° C ($3.52\times10^{-4}$ at 340° F) |
| Bearing cavity ambient pressure, N/$cm^2$ abs (psia) | 6.8 to 29 (10 to 42.6) |
| Bearing cavity ambient pressure at 6 $kW_e$, N/$cm^2$ abs (psia) | 17.8 (25.8) |

## JOURNAL BEARING

The cruciform tilting-pad journal bearing has the following geometric properties:

| | |
|---|---|
| Journal diameter at 21° C (70° F) at 0 rpm, cm (in.) | 4.4439 (1.7496) |
| Pad diameter at 21° C (70° F), cm (in.) | 4.4562 (1.7544) |
| Pad length, cm (in.) | 3.33 (1.312) |
| Pad arc length, rad (deg) | 1.92 (110) |
| Pivot location - percent of pad arc length from leading edge, percent | 65 |

The elastic properties of the cruciform are

| | |
|---|---|
| Radial direction, kg/cm (lb/in.) | $1.6\times10^4$ ($9.1\times10^4$) |
| Pitch and roll direction, m·kg/rad (in.-lb/rad) | 0.24 (21.1) |
| Yaw direction, m·kg/rad (in.-lb/rad) | 1.06 (92.0) |
| Flexure stiffness, N/m (lb/in.) | $350\times10^3$ (2000) |

The gas lubricated journal bearings are of the three-segment, tilting-pad type which are shown in figure 1. An external pressurization orifice and pocket is provided at each pad pivot axis to permit operation of the journal bearing during startup and shutdown.

Each of the three equally spaced pads in each journal bearing is pivoted by placing the foil (cruciform) in torsion. An exploded view of a pad and cruciform is shown in figure 2. The pivot location is 65 percent of the pad arc length measured from the leading edge. The pads are made of INCO-736X stainless maraging steel in the solution annealed condition. The cruciform element (fig. 3) is fabricated from INCO-736X cross-rolled plate that has been solution annealed and aged at 482° C (900° F). Basically, this concept involves attaching a thin beam to each end of a bearing pad with the beam passing over the pivot point. A second beam is attached to the first beam at a point located over the pivot point. This second beam is oriented at 90° to the first and is rigidly attached at its extremeties to the bearing support structure. The pitch motion of the pad will place the first beam in torsion. Roll motion will place the second beam in torsion. And yaw will put both beams in bending. Both beams are dimensionally deep in the radial direction and, therefore, stiff in that direction. Included in the journal bearing design is a provision for hydrostatic lift-off of each pad during startup, slow-speed operation, and shutdown. Hydrostatic lift-off is obtained by pressurizing a single hydrostatic orifice in each pad with jacking gas. Two of the bearing supports in each bearing are attached to solid beams (figs. 1 and 4) and are rigidly attached to the frame by means of the bearing carrier (fig. 4). The third bearing support is mounted to the frame by means of the bearing carrier through a resilient beam with a nominal spring rate of $350\times10^3$ newtons per meter (2000 lb/in.) (again, figs. 1 and 4). At assembly shims are installed between the resilient beam and the bearing carrier so that the bearing pad is

preloaded against the shaft. The shaft is clamped between the three pads with a preload of 16 to 23 newtons (8 to 12 lb). The low spring rate ($350 \times 10^3$ N/m (2000 lb/in.)) is used to accommodate differential growth, which tends to change bearing clearance. The growth is caused by thermal as well as centrifugal forces. Normal bearing ambient gas supply required to maintain the supply of the lubricant on the gas bearings is supplied by a bleed flow from the compressor discharge. The flow of the gas bleed is controlled by labyrinth seals at the turbine and compressor wheels, sized to limit the total bleed flow to 2 percent of the compressor flow.

### Thrust Bearing

The spiral-groove thrust bearing has the following geometric properties:

| | |
|---|---|
| Outside diameter, cm (in.) | 10.80 (4.25) |
| Inside diameter, cm (in.) | 5.3 (2.1) |
| Number of spiral grooves | 18 |
| Spiral angle, rad (deg) | 1.27 (72.9) |
| Inner radius of groove annulus, cm (in.) | 7.77 (3.06) |
| Groove-width to land-width ratio | 1.6 |

The gas-lubricated thrust bearing is of the spiral-grooved type and is shown in figures 1 and 5. Externally pressurized orifices (too small to be seen in fig. 5) are provided in each bearing stator plate to permit operation of the thrust bearing during start-up and shutdown.

The thrust bearing design consists of two flat plates bolted together at the periphery and separated by a spacer that is 100 micrometers (4 mils) thicker than the thrust runner. The bearing stator plates are made of annealed AISI 416 steel and are coated with approximately 50 micrometers (2 mils) of chromium oxide. The bearing surface of each plate contains 18 spiral grooves that are formed by masking the surface and then plasma spraying with chromium oxide.

## FLEXURE

The thrust bearing stator assembly is flexibly supported by four spokes from an outer member which locates and attaches the bearing assembly to the housing. The four-spoke, flexible-support member shown in figures 1 and 6 is a furnace-brazed subassembly consisting of an inner ring joined to an outer ring by brazing the spokes to that ring. To prevent buckling of the spokes due to differential expansion, they are

positioned tangentially to the inner and outer rings. With this configuration, differential expansion causes the inner ring to rotate relative to the outer ring, a motion which is acceptable to the design.

The angular stiffness of the flexure assembly is 220 newton-meters per radian (38 900 in.-lb/rad), approximately one-third of the tilt stiffness of the gas film at a load of 63 newtons (31 lbf). With this stiffness the flexure can accommodate 75 percent of the misalinement that may exist between the thrust runner and stator. However, this feature also results in a flexibility in the axial direction which is undesirable from the standpoint of retention of the axial clearance between the turbine and compressor wheels and their housings.

As reported in reference 2 during the initial testing of the flexibly supported spiral-groove thrust bearing, the performance of the thrust bearing in the hydrodynamic (self-acting) mode could not be evaluated because of a self-excited oscillation of the flexure. This flexure, chosen for its lack of wearing parts, is also lacking in dampening of the magnitude required for stable operation under BRU load conditions. The configuration in figure 6 uses a pair of spring beams rubbing members (fig. 7) located between the thrust bearing stator plate and the fixed ring of the flexure (fig. 8). These members add a frictional dampening moment of approximately 4.6 newton-meters (4 in.-lb).

## APPARATUS

The apparatus and instrumentation used to experimentally evaluate the cruciform-mounted journal bearing and the damped spiral-groove thrust bearing were identical to that used for evaluating the nonconforming pivoted-pad bearing evaluation, and a detail description of the apparatus and instrumentation is given in the text of that report (ref. 2).

## PROCEDURE

The initial step in testing the cruciform-mounted tilting-pad journal bearing and the damped spiral-groove thrust bearing was to establish the hydrostatic jacking gas flow characteristics of the bearings. Rotation was then started and gradually increased until the rated speed of 36 000 rpm was reached. At 36 000 rpm the hydrostatic jacking gas was gradually turned off, at which time the bearings were completely self-acting. Once the bearings become self-acting, the housing pressure was adjusted for the 6-electrical-kilowatt ($kW_e$) power level and run to reach thermal stability. The 6-$kW_e$ reference power level was used in this investigation to be consistent with the original BRU design specification. Off-design performance of the BRU was to range from a 2.25- to 10.5-

kilowatt net electrical output based on a reference output design of 6 $kW_e$.

## DISCUSSION OF RESULTS

### Hydrostatic Performance

Flow rate. - Design information for jacking gas systems is provided by measuring bearing gas flow rate at zero speed. The supply pressure to the bearings ranged from 55 to 103 newtons per square centimeter absolute (80 to 150 psia) in increments of 6.8 newtons per square centimeter absolute (10 psia) at a constant temperature of 300 K (540° R). The bearing cavity (simulator housing) pressure was regulated to two pressure levels at a constant inlet temperature of 300 K (540° R): 10.2 and 17 newtons per square centimeter absolute (15 and 25 psia). The two cavity pressure levels were used in this investigation since preliminary hydrostatic testing showed that the shaft would not lift off the journal bearings with cavity pressures higher than 13 newtons per square centimeter absolute (20 psia) within the range of jacking gas pressures considered. Figure 9 is a plot of the gas flow to the turbine journal bearing over the range of bearing pressures tested for the two cavity pressure. At normal bearing supply pressure of 103 newtons per square centimeter absolute (150 psia) and the simulated 6-$kW_e$ power level, the flow to the turbine journal bearing is 0.33 gram per second ($0.73\times10^{-3}$ lb/sec). Also shown in figure 9 is a point where the bearing is free from the journal for this one specific cavity pressure level. At this condition and any higher jacking gas pressure level, the shaft can rotate. At the reference cavity pressure level of 17.2 newtons per square centimeter absolute (25 psia) and with the simulator vertically oriented, the shaft would not lift off the bearings within the jacking gas pressure range tested. The argon gas flow is shown in figure 10 as it was determined for the thrust bearing, using the same supply pressure range that was used for the journal bearing. At the reference 6-$kW_e$ power level and normal thrust bearing gas supply pressure, the flow is 0.67 gram per second ($1.47\times10^{-2}$ lb/sec). Within the accuracy and the location of the instrumentation, no significant difference in flow to the thrust bearing was measured for the variations in the cavity pressure level covered in this test. The total flow of the thrust and journal bearings is presented in figure 11. At 103 newtons per square centimeter absolute (150 psia) bearing supply pressure and the reference 6-$kW_e$ power level, the flow is 0.32 gram per second ($1.8\times10^{-2}$ lb/sec) measured at the inlet lines to the housing.

Associated with the jacking gas flow to the bearing is the requirement that the jacking gas source supply maintain a high enough gas pressure between the bearing pad and the shaft to lift the shaft off the bearing. Along with sufficient gas flow the jacking gas system must supply gas pressure for a pressure ratio across the bearing

that is both compatible with the Brayton cycle and capable of lifting the shaft. Pressure ratio defined herein is the ratio of the bearing supply pressure to the housing pressure measured at the inlet fittings to the simulator housing. The cruciform bearing system did not lift readily during the hydrostatic testing of the system. With 36- to 38-newton (8- to 8.5-lb) bearing preload, the shaft cannot lift with a cavity pressure greater than 13.6 newtons per square centimeter absolute (20 psia). Although these data are good only for this particular configuration, this test has shown that the jacking gas lines to the bearing pad need to be redesigned to achieve lower line losses. The losses can be reduced by using a larger line and by increasing the jacking gas pad area.

Bearing film. - Measurements of hydrostatic (nonoperating) film thickness as a function of bearing cavity (housing) pressure are presented in figure 12. For normal hydrostatic operation of 103 newtons per square centimeter absolute (150 psia) bearing gas supply pressure and 17 newtons per square centimeter absolute (25 psia) cavity pressure, the film thickness at a turbine fixed journal pad is approximately 17 micrometers (0.67 mil).

The gas film between the thrust runner and the compressor thrust stator is less than the gas film on the turbine side of the bearing with a vertical orientation of the simulator and the turbine end up. Figure 13 shows that in the hydrostatic operation and with the dynamic simulator for the reference condition (bearing supply pressure, 103 $N/cm^2$ abs (150 psia); housing pressure level, 6-$kW_e$ (or 25 psia)) the films are 28 and 79 micrometers (1.1 and 3.1 mils) for the compressor and turbine sides, respectively. The difference in the film is caused by the direction of the load. The primary hydrostatic load is the rotor weight only toward the compressor.

## Hybrid Performance

Hybrid is defined herein as that condition under which the thrust and journal bearings are externally supplied with gas lubricant, the machine is running at some known speed, and the housing is pressurized.

Bearing transient performance. - During startup and shutdown, journal bearing critical speeds are encountered. The BRU is designed to pass through the first and second critical speeds and to operate between the second and third critical speeds. In the critical speed regions large increases occur in the shaft orbit. The size of the orbit depends on the amount of shaft unbalance and on the rate of acceleration or deceleration. The largest orbits occur during shutdown because of the slow rate of deceleration.

Figure 14 shows the turbine and compressor orthogonal traces as displayed on the oscilloscopes during shutdown. The upper two oscilloscope traces (figs. 14(a) and (b)) give the critical speeds at approximately 4770 rpm; the turbine and compressor shaft orbits are 25 and 30 micrometers (1.0 and 1.2 mils), respectively. The lower two

oscilloscope traces (figs. 14(c) and (d)) are of critical speeds occurring at 5580 and 6500 rpm for the turbine and compressor ends, respectively. The turbine orbit reaches a maximum amplitude of 22 micrometers (0.85 mil), and the compressor orbit reaches an amplitude of 13 micrometers (0.5 mil).

Thrust bearing - flexure. - The transient performance of the thrust bearing flexure was stable from zero to rated speed. The flexure motion relative to the housing is measured by capacitance probes (W and X), the location of which is shown diagrammatically in figure 9 of reference 2. The motion of the thrust bearing assembly for the hybrid mode of operation is shown in figure 15. Figure 15(a) shows the motion of the compressor and turbine sides of the thrust runner (porbes Q and R). Figure 15(b) shows the relative to the motion of the flexure (probes W and X). The hybrid mode is stable with very little motion of the flexure relative to the housing transmitted by the thrust rotor.

## Hydrodynamic Performance

Bearing component motion. - During the transition period from hybrid to hydrodynamic operation, while operating at rated speed, the oscilloscope traces showed no measurable change in size or wave form. Figure 16 shows oscilloscope traces of the shaft motion taken after the journal bearings were self-acting and thermally stable.

The compressor bearing orbit and its corresponding time-base trace are shown in figure 16(a). Each small vertical division of the grid is equal to 2.5 micrometers (0.1 mil). The orbit is slightly elliptical with a major axis of 4.5 micrometers (0.18 mil), which is consistent with other BRU and BRU simulator assemblies and is representative of the degrees of unblance.

The turbine bearing orbit is shown in figure 16(b). The orbit is circular with an axis of 2.5 micrometers (0.1 mil). The time-base traces of both orthogonal probes (C and D) are sinusoidal.

Figure 17(a) shows the motion of the leading edge of the turbine flexibly mounted pad. The amplitude of motion of the pad is not measurable.

The traces in figure 17(b) are roll motion of the flexible mounted journal pads. Roll motion is the tilting of the pad in the direction of the axis of the shaft (as shown in ref. 2) and normally is detected with two capacitance probes. During the assembly of this unit, however, one of the compressor probes became inoperative. The top trace, then, is the counterpart of this inoperative capacitance probe. The two bottom traces show the motion of the turbine pad. The roll motion of the bearing pads is small and is considered to be insignificant.

Figures 17(c) and (d) show the gas film of the compressor and turbine fixed mounted pads measured at the pivot line of the pad; its location is shown schematically in figure 10 of reference 2. The grid line marked 0 is the output value of the capacitance

probe when the shaft is at rest and in contact with the journal pad. The vertical distance from the datum line 0 to the oscilloscope trace is the measurement of the gas film thickness at the pivot line of the pad. For example, the film thickness for pad F at the pivot line is 10 micrometers (0.4 mil).

Figure 18 shows oscilloscope traces of both the motion and the gas film thicknesses of the loaded Q and unloaded R sides of the thrust of the bearing and the motion of its flexure (W and X). A more detailed description of the location of these capacitance probes can be found in reference 2. Figure 18(a) shows the hydrodynamic gas film thicknesses of the thrust bearing on both sides of the double acting thrust bearing operating at the 6-$kW_e$ power level. The total static axial clearance of the thrust bearing was mechanically measured to be 106 micrometers (4.2 mils). The grid lines marked Q and R in the photograph are the capacitance output values when the rotor is in the static position. In the static position with the turbine end of the simulator up and the axis of rotation in the vertical position, the rotor is in contact with the compressor side of the thrust bearing stator and has a value of Q equal to zero. In this position all the axial clearance is on the other side of the rotor, then R is equal to the total clearance of 106 micrometers (4.2 mils). The hydrodynamic thrust bearing gas film thickness for the 6-$kW_e$ power level is 15 and 7.9 micrometers (0.6 and 3.1 mils) for the compressor and turbine sides, respectively. It appears that the thermal growth and runout of the thrust rotor is 12.7 micrometers (0.5 mil).

Figure 18(b) shows oscilloscope traces of the output flexure probes (W and X) showing the motion of the damped flexure during the hydrodynamic mode of operation. The motion of the flexure is stable, small in amplitude and is considered to be insignificant.

Bearing temperatures. - The bearing temperatures reached in the simulator during ambient testing generally closely match the temperature obtained during hot operation of an actual BRU at the 6-$kW_e$ power level. Table I of reference 2 describes the locations of the thermocouples used and the temperatures measured for these locations during the cold-spin test, along with a few actual temperatures recorded from a hot BRU operation reported in references 5 and 6. The maximum temperature of 199° C (390° F) was reached on the compressor side (loaded) of the thrust bearing.

## SUMMARY OF RESULTS

The results of cold-spin testing of cruciform tilting-pad journal bearings and a damped flexibly mounted spiral-groove thrust bearing designed as an alternate bearing for the BRU are summarized as follows:

1. The pressure ratio required to lift this shaft off the bearing pads is in the order of magnitude of 6 to 7 times greater than that required for either the prototype or nonconforming pivoted-pad journal bearing.

2. The performance of the cruciform tilting-pad journal bearing was similar to that of the prototype fully conforming pivoted-pad journal bearing at the 6-electrical-kilowatt ($kW_e$) power level.

3. During the transition period from hybrid to hydrodynamic operation, the oscilloscope traces of the journal bearing motion showed no measurable changes in the size of the motion or in the wave shape.

4. At rated speed the largest shaft orbit diameter was approximately 4.5 micrometers (0.18 mil).

5. Gas film thickness of the fixed turbine pad was 13 micrometers (0.5 mil) at rated speed.

6. Gas film thickness of the loaded side of the thrust bearing was 15 micrometers (0.6 mil).

7. The damped thrust bearing was stable at rated speed, thus requiring only a small increase in inertia to dampen out the inherent instability (see ref. 2).

8. The temperature distribution for the bearing system was essentially the same as that of a hot Brayton cycle rotating unit, with the exception of the loaded side of the thrust bearing, which was 199° C (390° F).

Lewis Research Center,
National Aeronautics and Space Administration,
Cleveland, Ohio, November 1, 1973,
502-25.

## REFERENCES

1. Frost, A.; Tessarzik, J. M.; Arivas, E. B.; and Waldron, W. D.: Design and Fabrication of Gas Bearings for Brayton Cycle Rotating Unit. Rep. MTI-72TR34, Mechanical Technology, Inc. (NASA CR 121098), Mar. 1973.

2. Ream, L. W.: Performance of Gas-Lubricated Nonconforming Pivoted-Pad Journal Bearings and a Flexibly Mounted Spiral-Groove Thrust Bearing. NASA TM X-2765, 1973.

3. Klann, J. L.: 2 to 10 Kilowatt Solar or Radioisotope Brayton Power System. Intersociety Energy Conversion Engineering Conference. Vol. 1. IEEE, 1968, pp. 407-415.

4. Davis, J. E.: Design and Fabrication of the Brayton Rotating Unit. NASA CR-1870, 1972.

5. Klassen, H. A.; Winzig, C. H.; Evans, R. C.; and Wong, R. Y.: Mechanical Performance of a 2 to 10 Kilowatt Brayton Rotating Unit. NASA TM X-2043, 1970.

6. Johnsen, R. L.; Namkoong, D.; Edkin, R. A.: Steady-State Temperature Distribution Within Brayton Rotating Unit Operating in a Power Conversion System Using Helium-Xenon Gas. NASA TM X-67990, 1971.

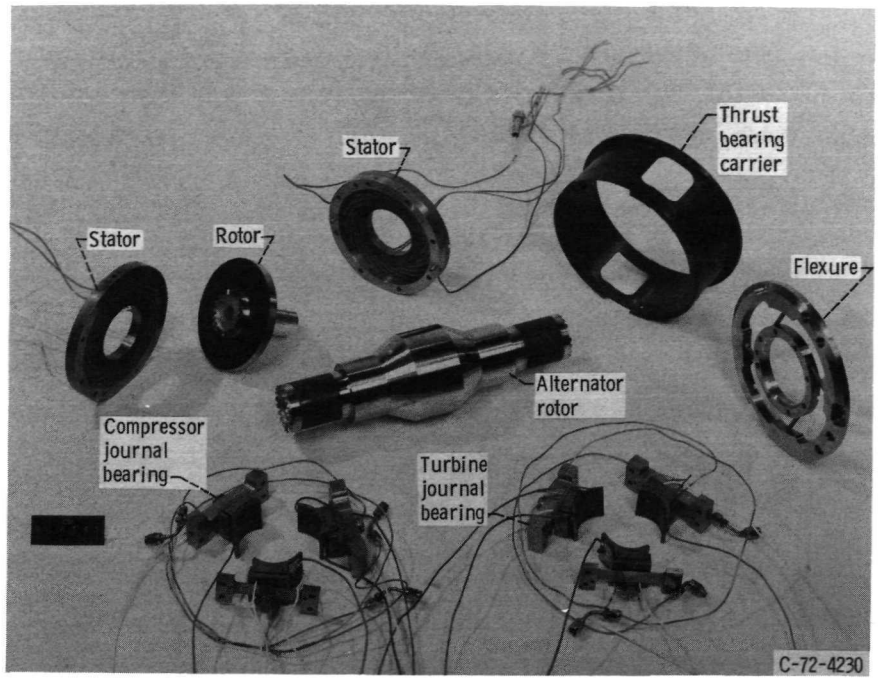


Figure 1. - Gas bearing system.

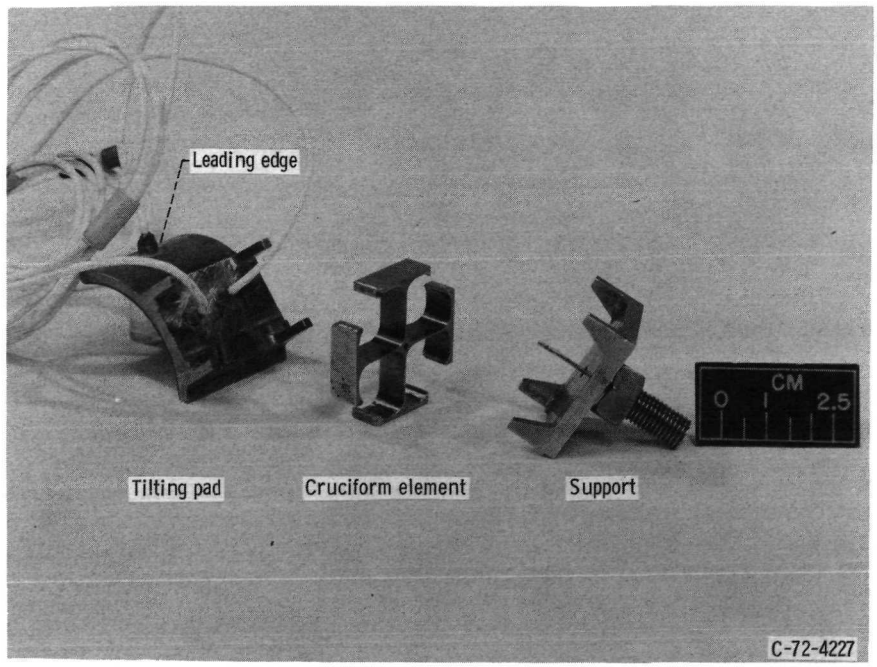


Figure 2. - Exploded view of cruciform tilting pad.

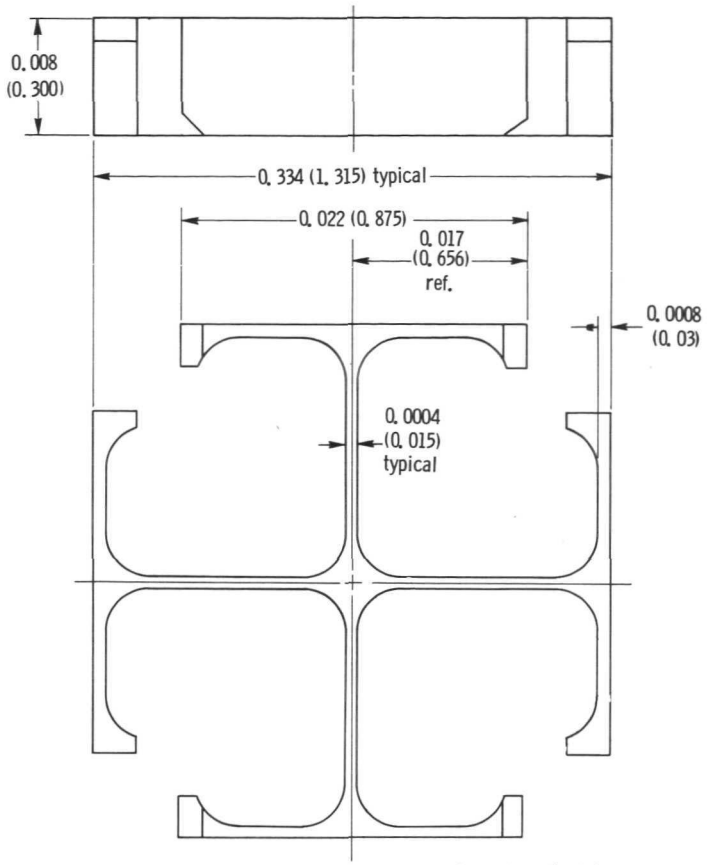


Figure 3. - Cruciform. (Dimensions are in meters (in.).)

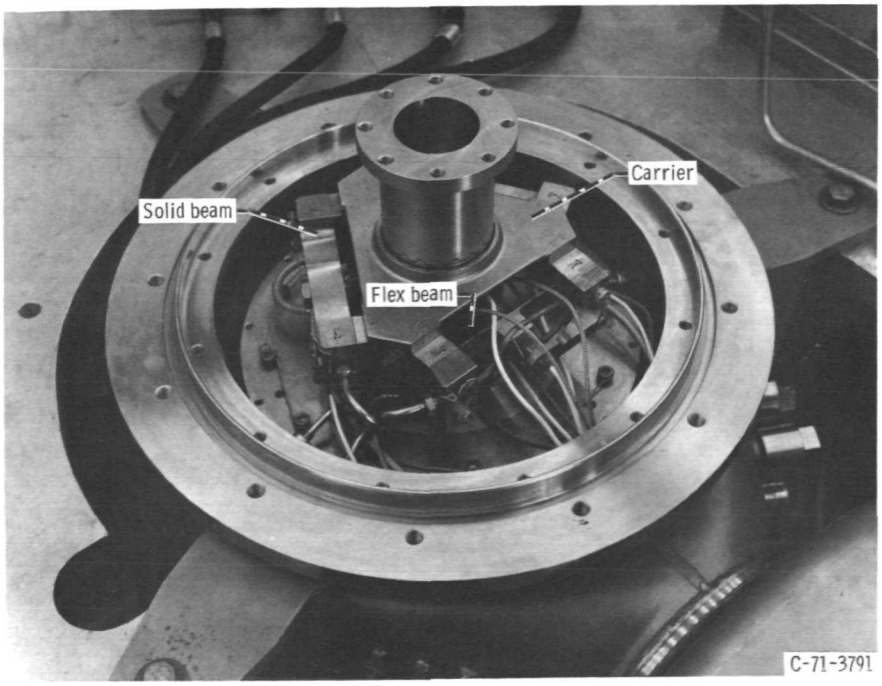


Figure 4. - Journal bearing installed in simulator.

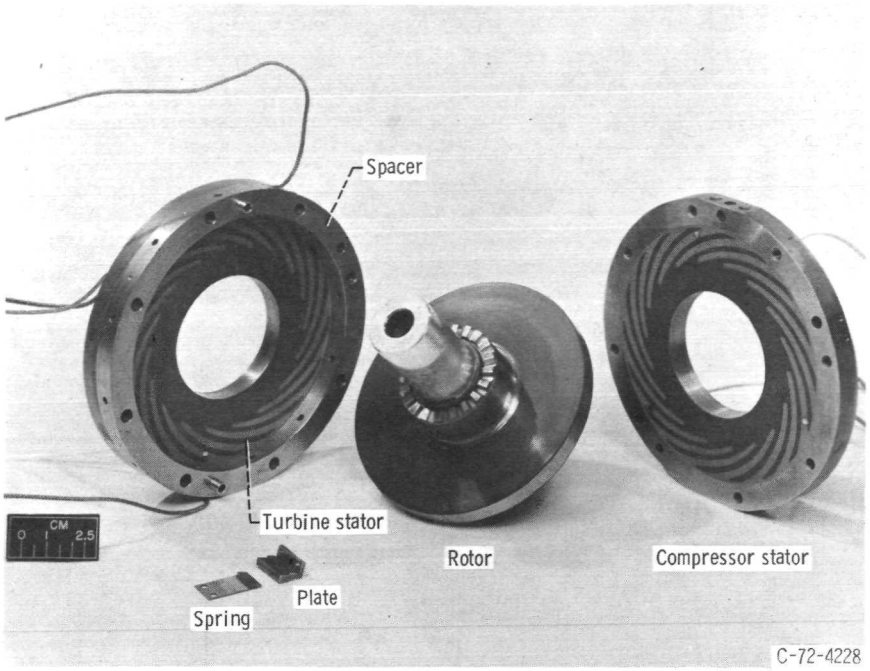


Figure 5. - Spiral grove thrust bearing.

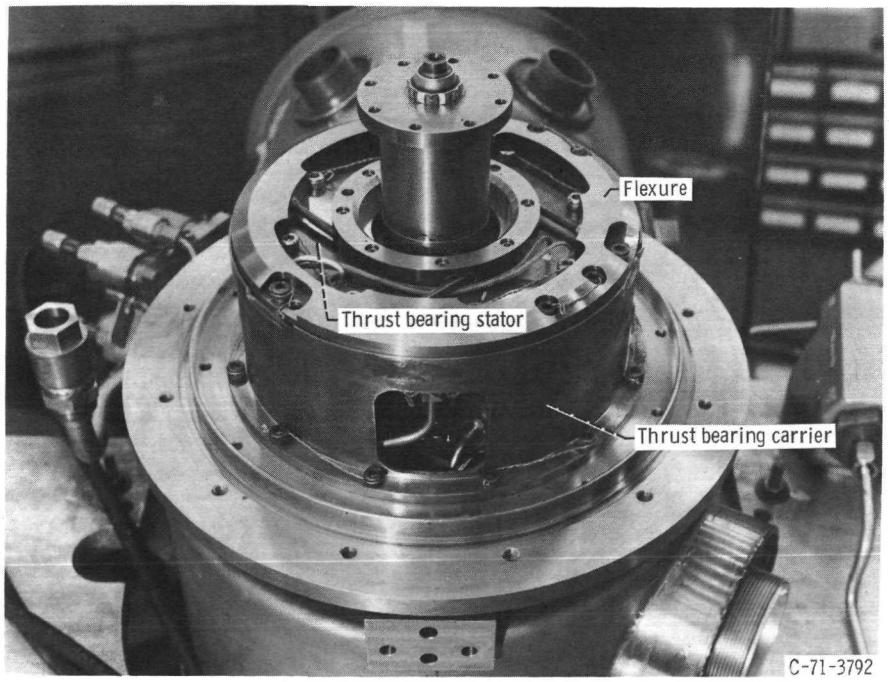


Figure 6. - Thrust bearing installed in simulator.

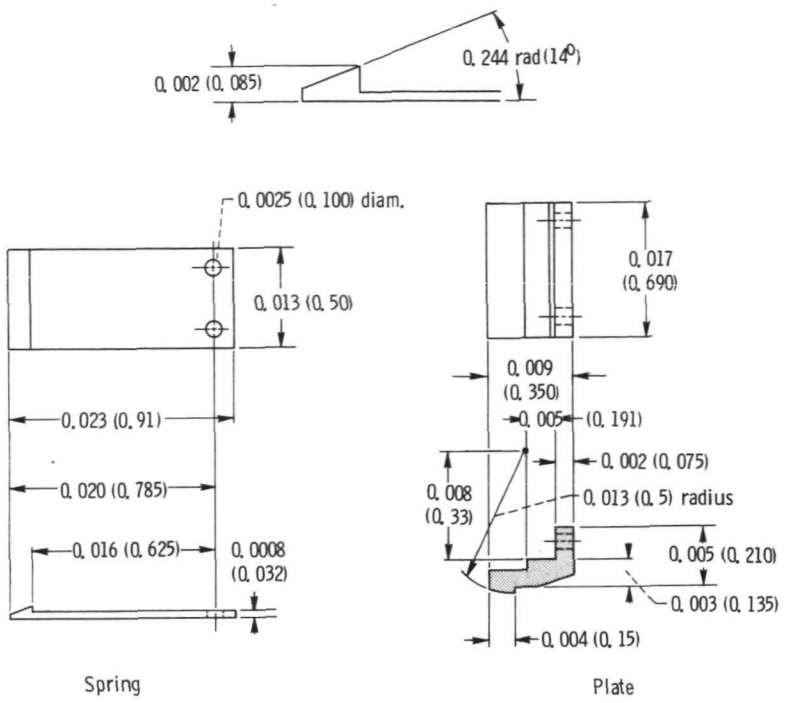


Figure 7. - Flexure damper. (Dimensions are in meters (in.).)

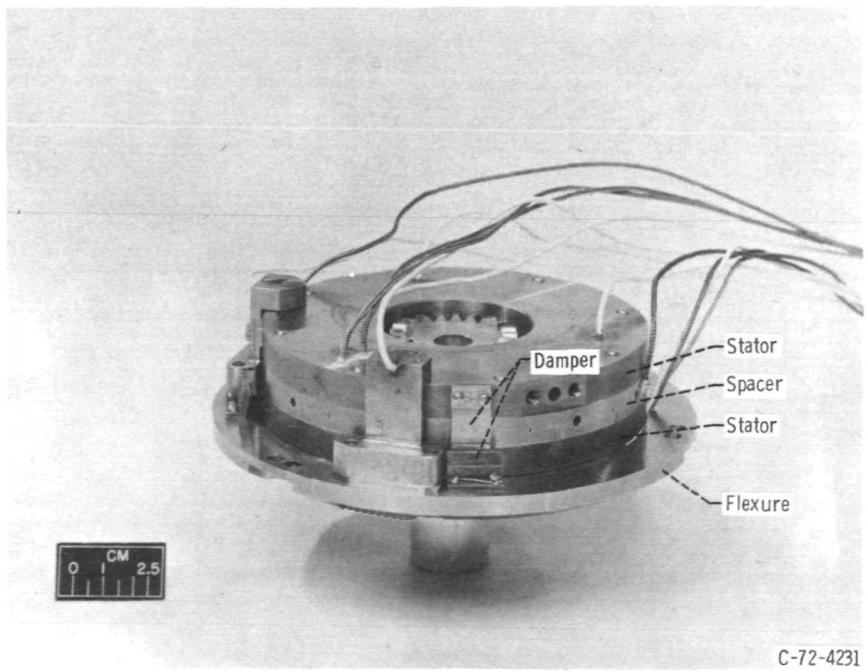


Figure 8. - Thrust bearing subassembly.

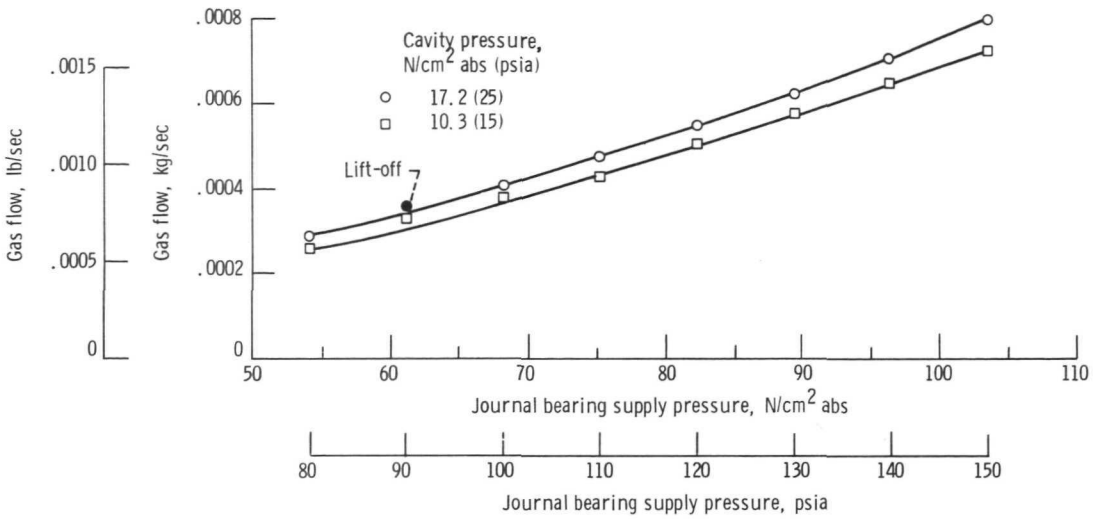


Figure 9. - Gas flow to turbine journal bearing.

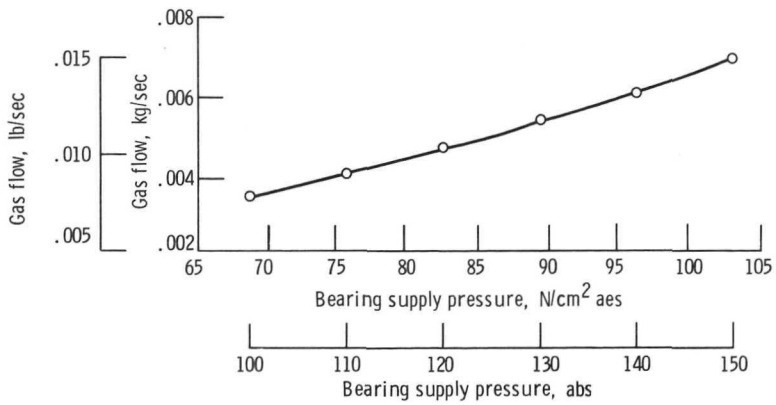


Figure 10. - Total gas flow to thrust bearing.

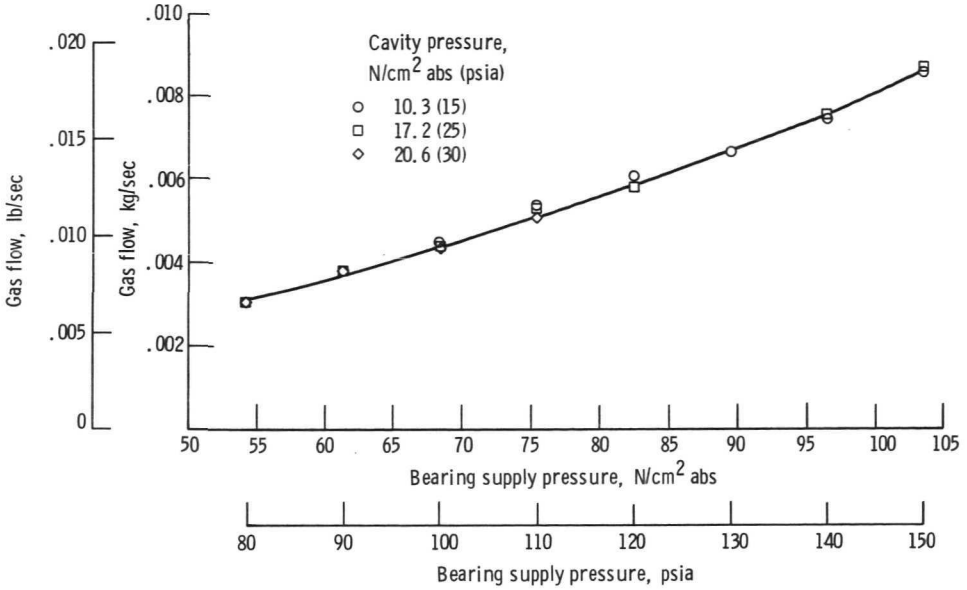


Figure 11. - Total gas flow to bearings.

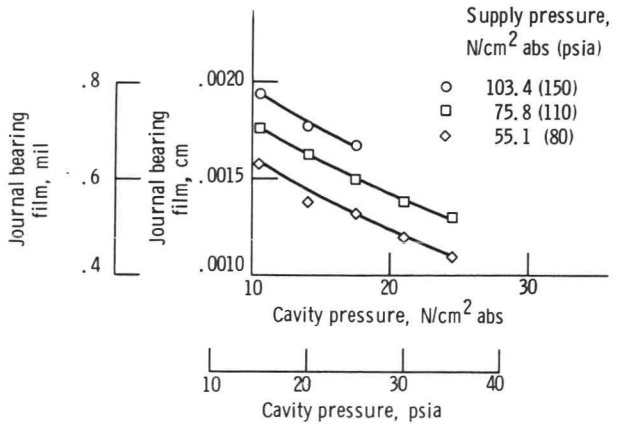


Figure 12. - Hydrostatic journal bearing film.

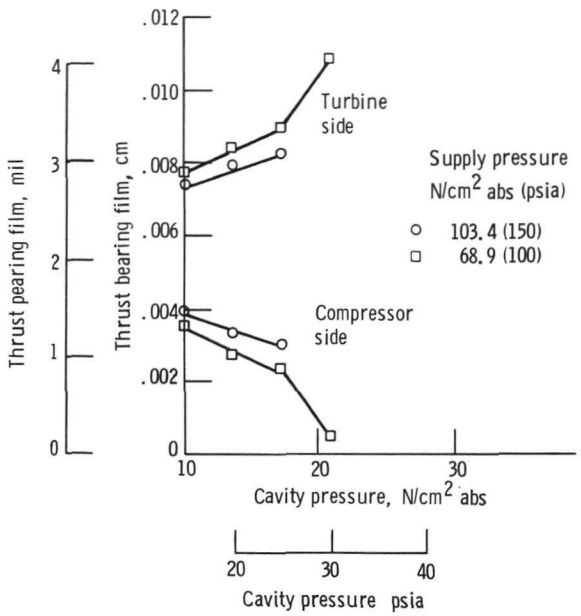


Figure 13. - Hydrostatic thrust bearing film.

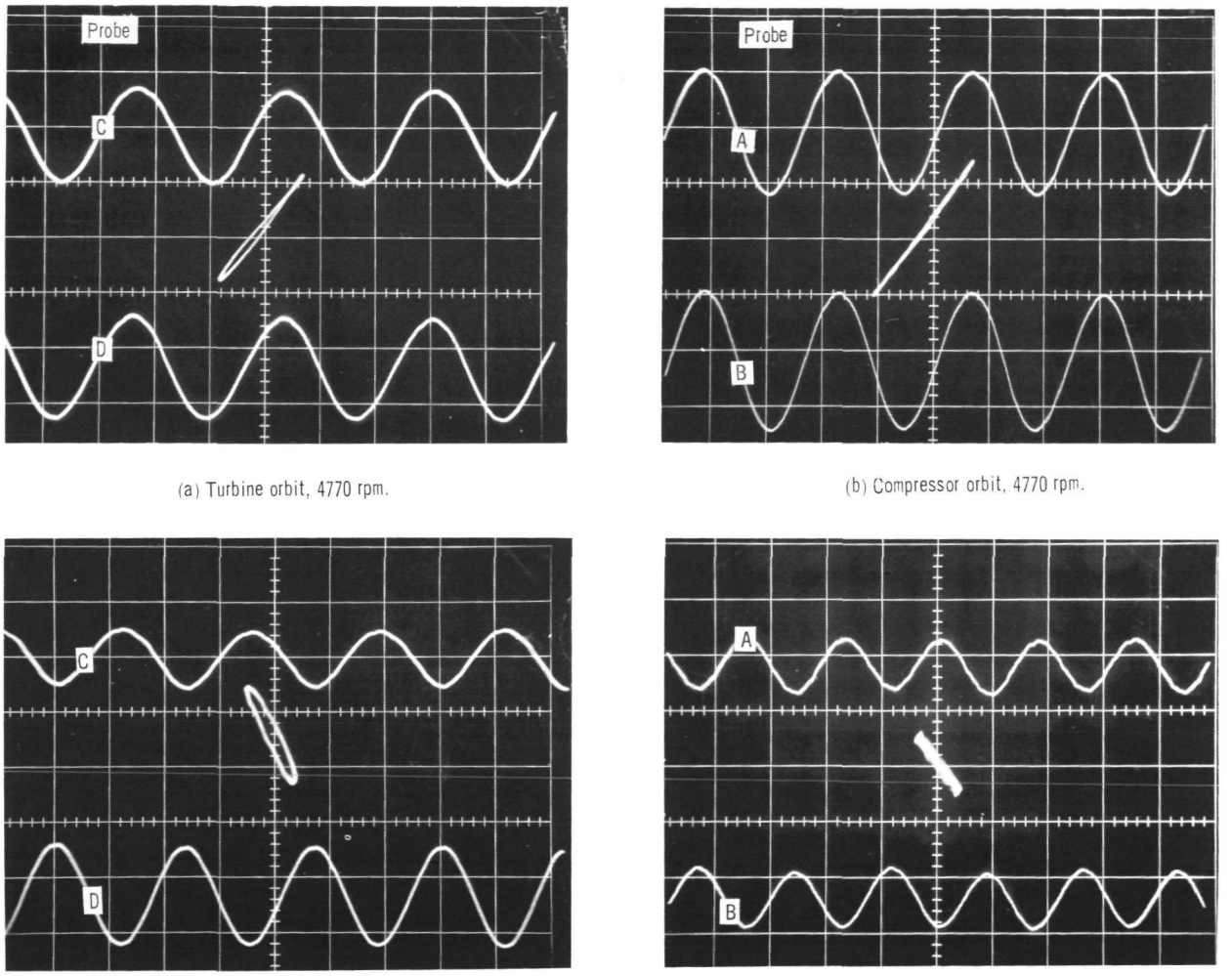


(a) Turbine orbit, 4770 rpm.

(b) Compressor orbit, 4770 rpm.

(c) Turbine orbit, 5580 rpm.

(d) Compressor orbit, 6500 rpm.

Figure 14. - Critical speed. Cavity pressure, 17.3 newtons per square centimeter absolute (25 psia); thrust and journal bearing supply pressure, 103.4 newtons per square centimeter absolute (150 psia). Time scale, 2 milliseconds per division; amplitude scale, $0.25 \times 10^{-3}$ centimeter (0.1 mil) per division.

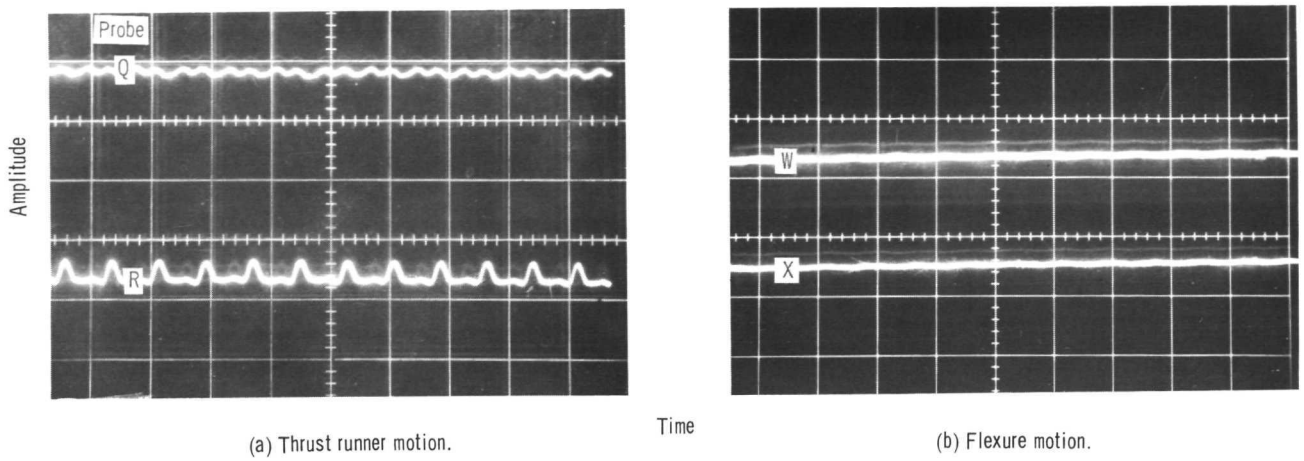


(a) Thrust runner motion.

(b) Flexure motion.

Figure 15. - Thrust bearing assembly motion. Cavity pressure, 17.3 newtons per square centimeter absolute (25 psia); thrust and journal supply pressure, 103.4 newtons per square centimeter absolute (150 psia); speed, 36 000 rpm. Time scale, 2 milliseconds per division; amplitude scale, $0.25X10^{-3}$ centimeter (0.1 mil) per division.

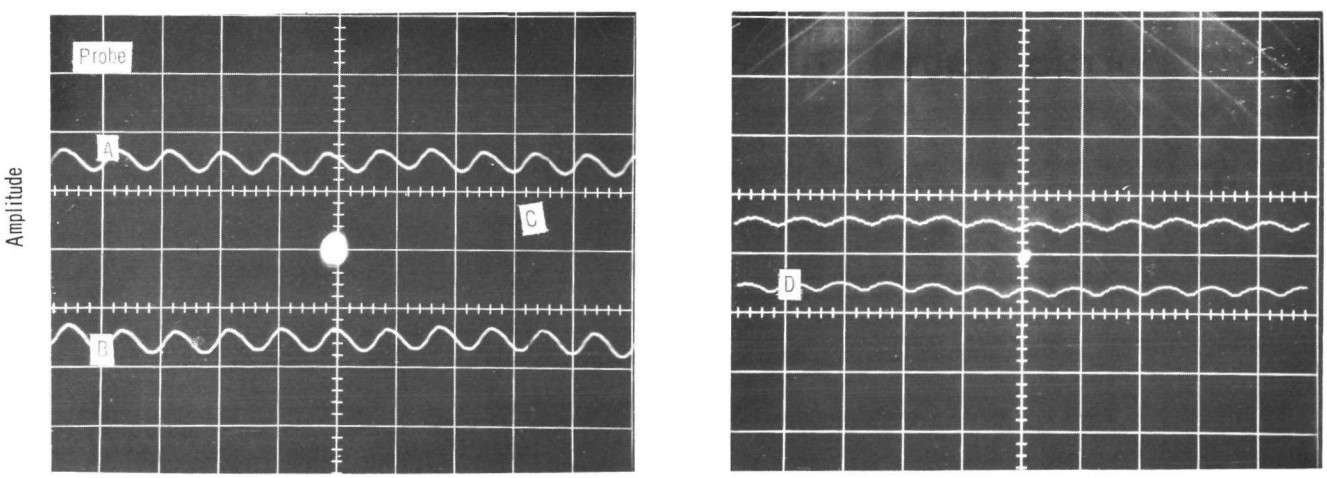


(a) Compressor bearing journal orbit.

(b) Turbine bearing journal orbit.

Figure 16. - Shaft motion. Cavity pressure, 17.3 newtons per square centimeter absolute (25 psia); thrust and journal bearings self-acting; speed, 36 000 rpm. Time scale, 2 milliseconds per division; amplitude scale, $0.25X10^{-3}$ centimeter (0.1 mil) per division.

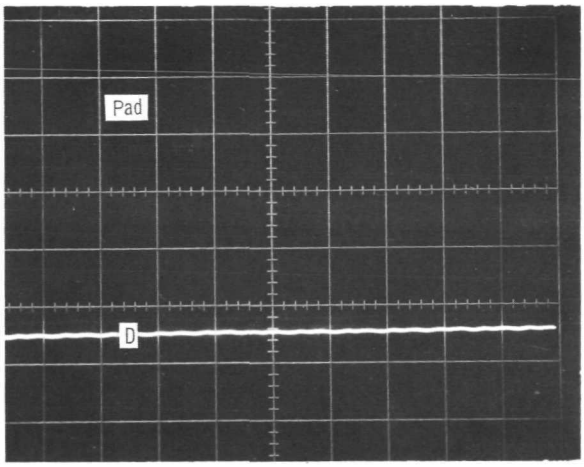


(a) Leading-edge motion; flexibly mounted turbine journal pad.

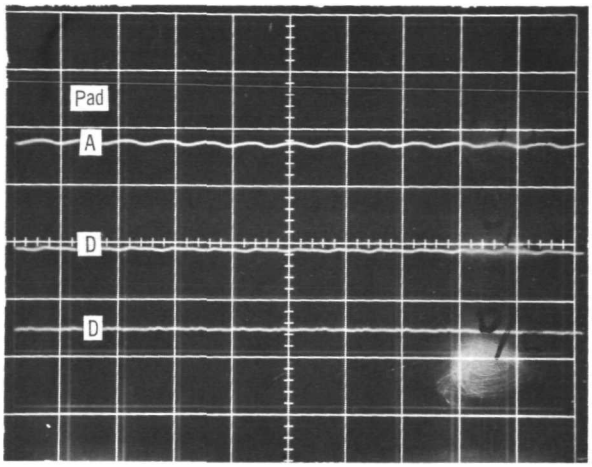


(b) Roll motion; flexibly mounted journal pads.

Amplitude

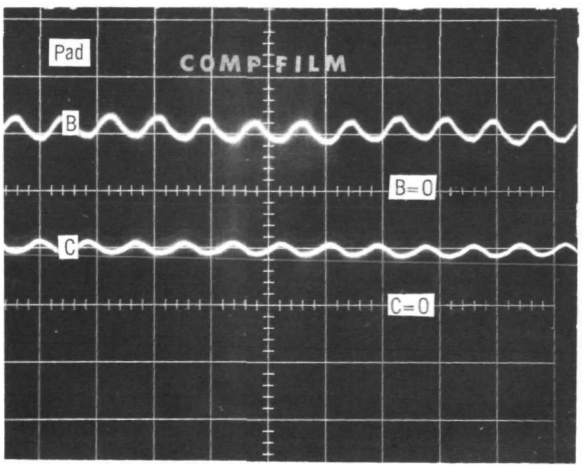


(c) Gas film; compressor journal fixed pad bearings.

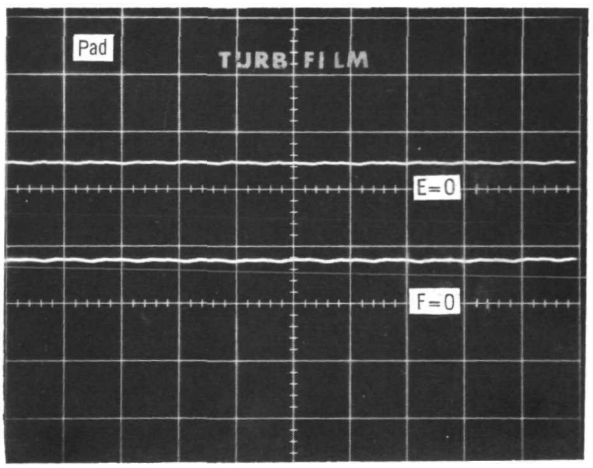


(d) Gas film; turbine journal fixed pad bearings.

Time

Figure 17. - Journal bearing motion and gas film. Cavity pressure, 17.3 newtons per square centimeter absolute (25 psia); thrust and journal bearings self-acting; speed, 36 000 rpm. Time scale, 2 milliseconds per division; amplitude scale, 0.25X10-3 centimeters (0.2 mil) per division.

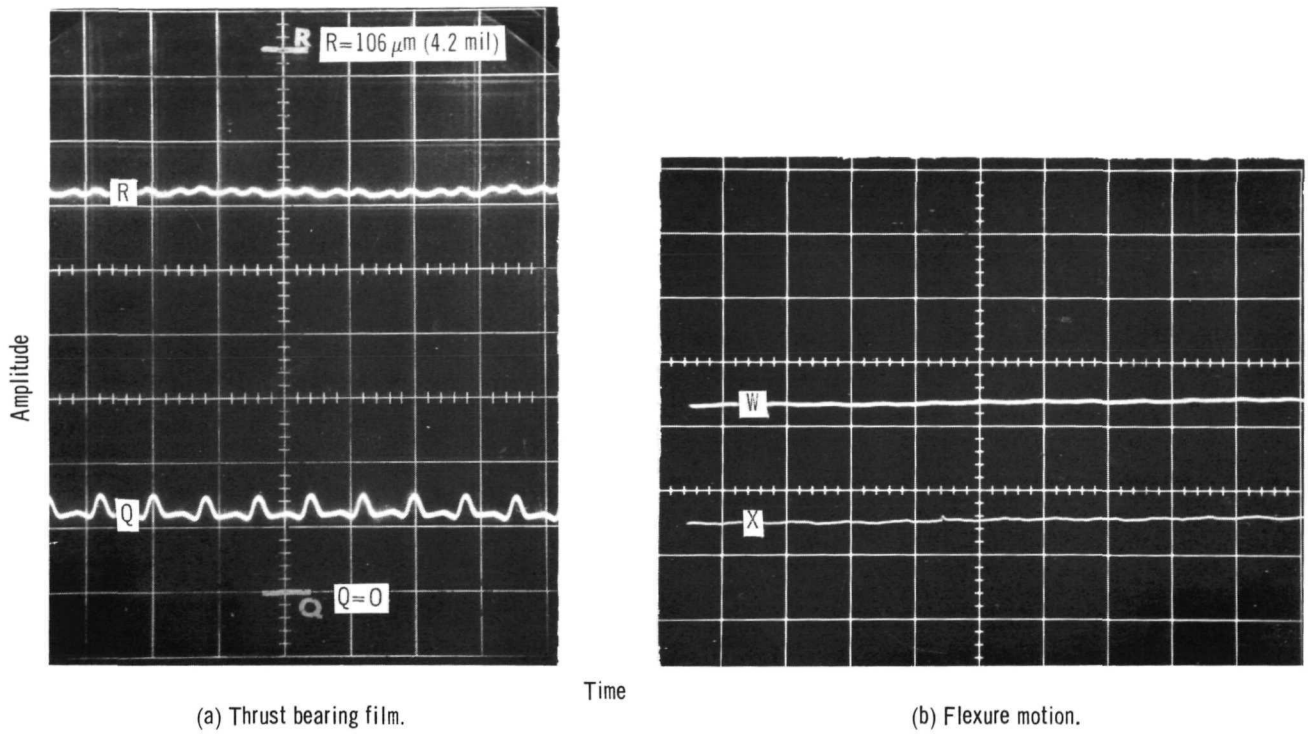


(a) Thrust bearing film.

(b) Flexure motion.

Figure 18. - Thrust bearing film and flexure motion. Cavity pressure 17.3 newtons per square centimeter absolute (25 psia); thrust and journal self-acting. Time scale, 2 milliseconds per division; amplitude scale, 1 minor division, $0.25 \times 10^{-3}$ centimeter (0.1 mil).



NASA-Langley, 1974 E-7675

NATIONAL AERONAUTICS AND SPACE ADMINISTRATION
WASHINGTON, D.C. 20546

OFFICIAL BUSINESS
PENALTY FOR PRIVATE USE $300

SPECIAL FOURTH-CLASS RATE
BOOK

POSTAGE AND FEES PAID
NATIONAL AERONAUTICS AND
SPACE ADMINISTRATION
451

U.S.MAIL

POSTMASTER : If Undeliverable (Section 158 Postal Manual) Do Not Return

*"The aeronautical and space activities of the United States shall be conducted so as to contribute . . . to the expansion of human knowledge of phenomena in the atmosphere and space. The Administration shall provide for the widest practicable and appropriate dissemination of information concerning its activities and the results thereof."*

—NATIONAL AERONAUTICS AND SPACE ACT OF 1958

# NASA SCIENTIFIC AND TECHNICAL PUBLICATIONS

TECHNICAL REPORTS: Scientific and technical information considered important, complete, and a lasting contribution to existing knowledge.

TECHNICAL NOTES: Information less broad in scope but nevertheless of importance as a contribution to existing knowledge.

TECHNICAL MEMORANDUMS: Information receiving limited distribution because of preliminary data, security classification, or other reasons. Also includes conference proceedings with either limited or unlimited distribution.

CONTRACTOR REPORTS: Scientific and technical information generated under a NASA contract or grant and considered an important contribution to existing knowledge.

TECHNICAL TRANSLATIONS: Information published in a foreign language considered to merit NASA distribution in English.

SPECIAL PUBLICATIONS: Information derived from or of value to NASA activities. Publications include final reports of major projects, monographs, data compilations, handbooks, sourcebooks, and special bibliographies.

TECHNOLOGY UTILIZATION PUBLICATIONS: Information on technology used by NASA that may be of particular interest in commercial and other non-aerospace applications. Publications include Tech Briefs, Technology Utilization Reports and Technology Surveys.

***Details on the availability of these publications may be obtained from:***

**SCIENTIFIC AND TECHNICAL INFORMATION OFFICE**

**NATIONAL AERONAUTICS AND SPACE ADMINISTRATION**

**Washington, D.C. 20546**